

---

## Results of Investigation Forward and Backward Extrusion with FEM Program QForm

Prepared by - B. Moroz<sup>1</sup>, S. Stebunov<sup>2</sup>, N. Biba<sup>2</sup>, K. Mueller<sup>3</sup>

1. Don State Technical University (DSTU), Russia
2. QuantorForm Ltd., Russia
3. Forschungszentrum Strangpressen, Technische Universitaet Berlin, Germany

**ABSTRACT** --- The paper presents finite-element model realized in QForm FE program for simulation of extrusion. It presents the forward, backward and active friction force extrusion simulation results. Dependence of the consideration for boundary conditions made it possible to obtain design material flow patterns in the container as a function of the value and direction of the friction forces between the billet and the container corresponding to the pilot data. We have analyzed the material flow features in pressing-out the billet in the container. We have obtained the distribution of contact pressures / normal stresses on the extruder plate, container and die surfaces during forward and backward extrusion. The software calculates the full extrusion force and its components with a high accuracy. It permits to define the thermal pattern in the billet considering its cooling in the air and during the contact to the tool, and to obtain the information of the stresses, strain and thermal state throughout the entire forming process not only in the billet being extruded, but in the points of interest for the researcher as well. We have stated the billet deformation features in the container and those of the backward extrusion force parameters change, which are testimony to the presence of active friction forces in the initial stage of the process. We have defined the most suitable conditions for the initial extrusion phase with friction forces acting vigorously in the specified kinematical conditions.

---

### I. Introduction

An all-round heterogeneous compression pattern and considerable billet strains are distinctive of the extrusion process as compared to the other plastic metal working techniques. Complexity in analyzing this process accounts for large numbers of experimental studies covering the material flow in the container, effect of various factors on the extrusion force, temperature and the deformed state of extrusion products obtained and the fact that the first publications in the extrusion theory field did not emerge until early 30's in the last century [1,2].

The theoretical study methods like a simultaneous solution of the equilibrium equation and the plasticity, slip lines, upper bound estimation and work balance condition permit to

define the forces expended for deforming a billet with a certain degree of accuracy. The viscoplasticity method based on experiments and theory opened new opportunities to the researchers, but it is too labor-consuming and does not suit to many extrusion applications.

Over the recent years, to study various plastic metal working techniques, the researchers began using numerical models based on the finite and boundary element methods, which consider non-linear material behavior and non-linear boundary conditions. A number of finite-element models have been developed, which are used to study the extrusion process [3-9]. However, the process being complex, simulation is limited to studying individual extrusion stages. It uses short billets. Consideration is given mainly to forward extrusion, assuming that the size of the plastic deformation area is localized [8]. The sources

published practically lack any data on the simulation of the entire process from pressing out the billet till the very end of the process.

This paper presents the forward, backward and active friction force (AFF) extrusion simulation results, using the QForm software comparing to experiments. Mathematical formulation and brief description of the program can be found in [10].

## II. Simulation objectives and conditions

The QForm software proved itself to be good for die forging process simulation and is widely used both for the preparation of production and training practice. It can also be used for short product extrusion process analysis. The positive initial billet extrusion stage simulation results [12] led to testing the software for studying the entire extrusion process for billets with two and more diameters in length. Calculations have been made for three extrusion techniques (Fig. 1): forward (a), backward (b) and AFF extrusion (c).

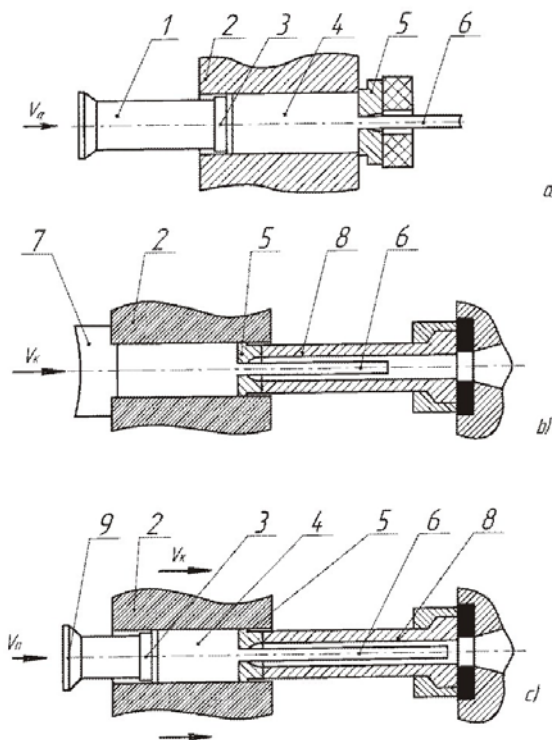


**Figure 1.** Extrusion arrangements for forward (a), backward (b) and active friction force extrusion (c): 1 – ram; 2 – container; 3 – extruder plate; 4 – billet; 5 – die; 6 – product; 7 – plug; 8 – hollow die holder; 9 – short ram.

To obtain a possibility of comparing the design data with the experiment, the following simulation conditions have been chosen: D16 (2024) aluminum alloy; the container diameter 110 mm, a drawing factor equal to 10.0; 390°C the billet temperature, 380°C container temperature, 390°C extruder plate and die temperature. Extrusion was without billet lubrication; billet cooling time 5 s in the air and 10 s in the container; 3 mm/s extrusion speed.

## III. Material flow in the container and extrusion force.

Fig. 2 shows the grid of flow lines at various forward extrusion stages. It follows from the figure on the right that the shape and size of the plastic deformation area at the die match the shape and size of the slip line field constructed for the conditions of the maximum friction between the billet and the tools.

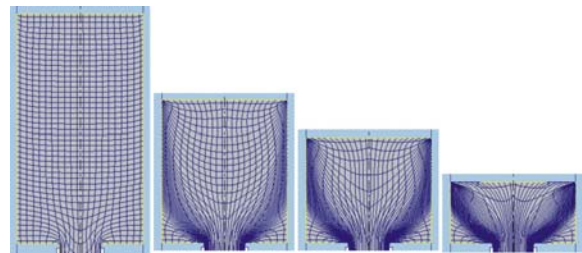


**Figure 2.** Flow lines grids for forward extrusion obtained by simulation. Butt-end length in the container from left to right: 202, 126, 93 and 54 mm respectively.

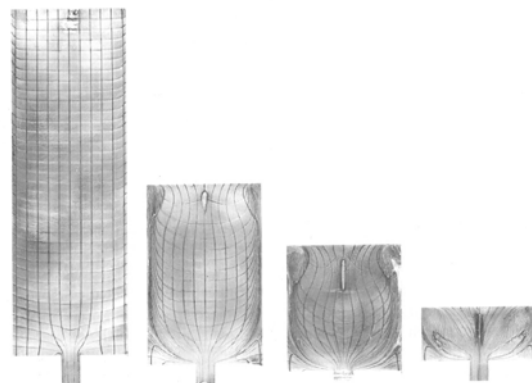


**Figure 3.** Material flow during forward extrusion obtained experimentally [9]: Initial billet length is 350 mm. Butt-end length from left to right: 333, 174, 122 and 55 mm respectively.

Comparing these data with the material flow patterns obtained experimentally (Fig. 3), we can see that they are closely related: in both cases the shearing deformations at the container and the shearing deformations in the dead area at the die grow as the billet reduces in length, and the characteristic material pinch areas at the extruder plate reveal become more and more clearly. Some differences in the coordinate grids deformation rate are accounted for by different initial billet lengths. At the same time we can notice an increase in the billet deformation and process non-steady-state non-uniformity as its initial length increases.

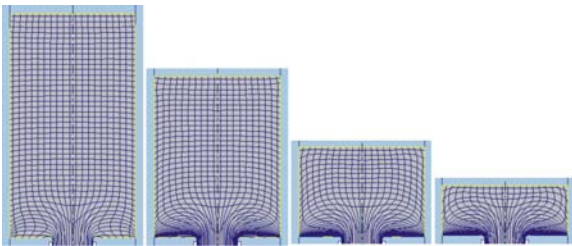


**Figure 4.** Flow lines for AFF extrusion. Butt-end length in the container from left to right: 199, 143, 76 and 44 mm.

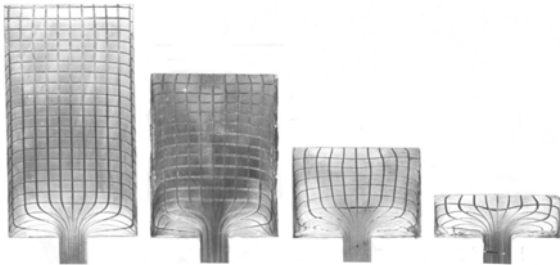
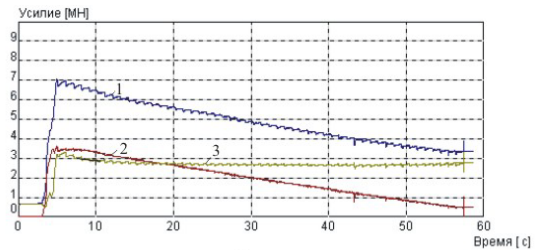


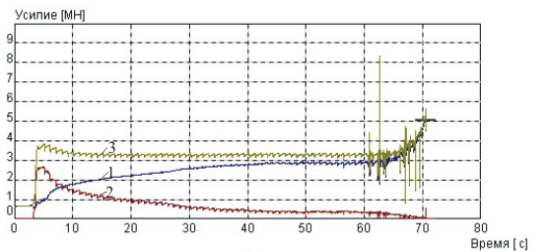
**Figure 5.** AFF extrusion material flow. Initial billet length is 280 mm. Butt-end length from left to right: 200, 140, 80 and 40 mm.

During AFF extrusion at the relative container movement speed value  $K_V = 1.4$  ( $K_V$  is the ratio between the  $V_K$  container movement speed and the  $V_T$  ram movement speed), the coordinate grid deformation is changing fundamentally (Fig. 4): there is no material pinch area at the extruder plate and a dead area at the die; the material at the extruder plate moves in the radial direction from the billet axis to the container; the active forces contribute to a larger reduction of the central billet layers in the deformation area, which is confirmed indirectly by the compressive deformations of the axial coordinate grid cells

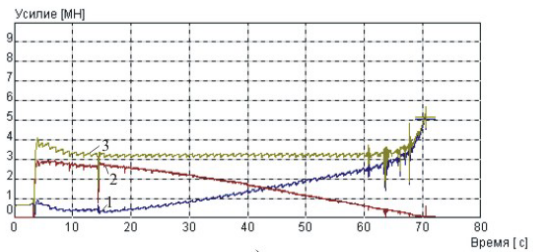
exterior to the plastic deformation area. The flow lines (Fig. 2 and 4) are in good agreement with the experimental ones (Fig. 3 and 5). It is worth noting that the design material flow at the billet-container contact surface is less intense than that obtained in the experiment, because sticking conditions occur during the extrusion of the 2024 alloy on the billet-tools contact surface, whereas slipping is assumed during simulation.



a)



b)



c)

**Figure 6.** Calculated force diagrams for forward (a), backward (b) and AFF extrusion (c): 1 – the force taken by the ram; 2 – friction force between the billet and the container; 3 – the force taken by the die. Butt-end height: 40mm (a), 8.8 mm (b,c).

The force diagrams (Fig. 6) are characteristic of the extrusion techniques in question. A merit of the QForm software is the possibility to obtain the information about the components of the full extrusion force. In any process phase under study the condition of the equality of the component sum to the full extrusion force is met: with the direct technique, the full force applied to the ram ( $F_T = F_{\Sigma}$ ) equals the sum of the friction forces between the billet and the container  $F_K$  and the force taken by the  $F_M$  die; during

backward extrusion and AFF extrusion  $F_M = F_{\Sigma} = F_K + F_{\Pi}$ .

The relationship among the full extrusion forces for the techniques under discussion corresponds to the data published [11]. For the set conditions the full backward extrusion force is by 44% lower than the forward extrusion force and by 10% lower than the AFF extrusion force. The design values of the full forces for backward extrusion and those for AFF extrusion do not exceed the experimental data by more than 10%. The force of friction between the billet and the container for AFF extrusion in the experiment was about 10% above the design value, because the container temperature in the latter case was by 30°C lower than that assumed for the calculations.

There are active friction forces during backward extrusion, especially in the initial process phase. Their presence during the extrusion of the billets with more than two diameters in length has been shown in the papers covering the initial extrusion stage studies [12 and 13] and is confirmed experimentally.

Hence the data quoted are testimony to the reliability of the material flow simulation results obtained for the extrusion by various techniques and that of the power input for the processes.

#### IV. Features of pressing-out in the container and contact pressure profiles.

When pressing-out a billet of an increased length in an irrational manner, the  $F_K$  friction force between the billet and the container can exceed the full AFF extrusion force. In this case, the material efflux will only begin due to the  $F_K$  friction forces with no pressure on the extruder plate. Hence it will be impossible to start AFF extrusion at the assigned  $V_K$  and  $V_{\Pi}$  velocities (see Fig. 1,c). To substantiate rational billet pressing-out conditions for AFF extrusion, this process phase has been considered in more detail. As the pressing-out of a billet may take place similar to forward or backward extrusion, depending on the extrusion pattern [12 and 13], both options has been considered.

Simulation of the initial extrusion phase has been done at the following conditions: billet diameter 105 mm, length 280 mm; 400°C billet

and container temperature; 2 mm/s ram speed; drawing ratio is 10.

During forward extrusion, after a contact of the billet being pressed out to the container (Fig. 7, b) it is first pressed out in the area adjacent to the extruder plate. Then the pressed out portion of the billet is shifted relative to the container, being consistently pressed out in the direction of the die (Fig. 7, c, d). The material efflux from the die channel begins after the billet has been pressed out in the container completely (Fig. 7, f).

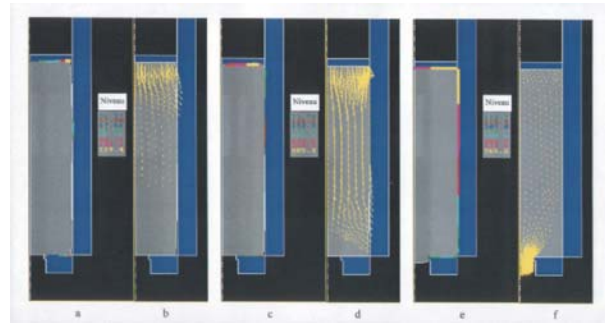


**Figure 7.** The billet-container contact surface, the value of the contact pressure on the tools (a, c, e) and the speed vector field (b,d,f) in the initial forward extrusion stage with a ram stroke of 18 mm (a,b), 22 mm (c,d) and 26 mm (e,f) [12].

During backward extrusion, on the contrary, after the billet touches the container, pressing-out starts in its portion facing the die (Fig. 8, b), because the friction forces between the billet and the container oppose its shift relative to the container. After pressing out the portion of the billet adjacent to the die, the portion of the billet already pressed out is shifted relative to the container (Fig. 8, d), overcoming the friction forces directed toward the die. The billet-container contact surface increases toward the extruder plate (Fig. 8, c, d) and, the forces  $F_K + F_{\Pi} = F_{\Sigma} = F_M$  being equal, the material efflux from the container begins (Fig. 8, e, f). At this time, there is a free lateral billet surface at the extruder plate, i.e. the billet has not been pressed out in the container completely, when the efflux begins. Its further pressing-out is only possible, if the pressed-out billet portion is displaced relative to the container.

Material flow is well seen from the distribution of the velocity components fields on Figs. 9,10.

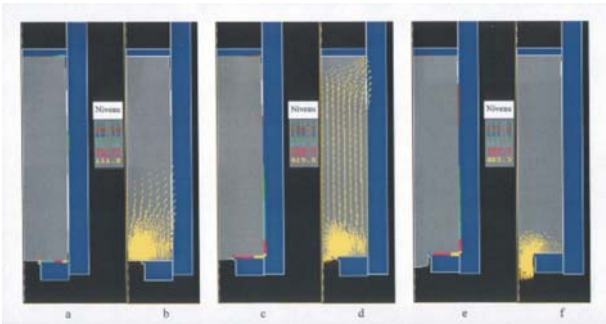


**Figure 8.** The billet-container contact surface, the value of the contact pressure on the tools (a, c, e) and the speed vector field (b,d,f) in the initial backward extrusion stage with a ram stroke of 18 mm (a,b), 22 mm (c,d) and 26 mm (e,f) [12].

From the data obtained it appears that during AFF extrusion the pressing-out of the billet in the container should be concluded so that the  $F_K < F_S$  condition is met, when the drive is activated and the movement with a pre-determined speed begins. The software offers a more detailed study of the material points flow in the billet along the X and Y axes in the phase when it is pressed out.

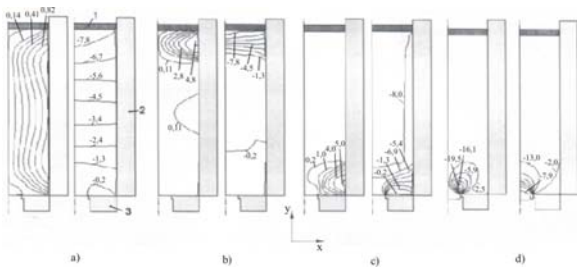


**Figure 9.** Constant value lines for radial (left figures) and axial (right figures) of the component velocities of material points in the initial forward extrusion stage: a – before the billet touches the container; b – after the billet has touched the container; c – before the material begins to flow from the container; d – at the beginning of the efflux; 1 – extruder plate; 2 – container; 3 – die.

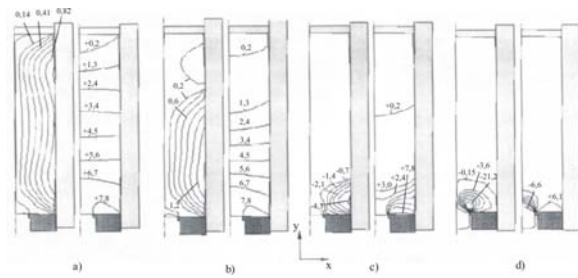


**Figure 10.** Constant value lines for radial (left figures) and axial (right figures) of the component velocities of material points in the initial backward extrusion stage: a – before the billet touches the container; b – after the billet has touched the container; c – before the material begins to flow from the container; d – at the beginning of the efflux; 1 – extruder plate; 2 – container; 3 – die.

The contact pressure profiles on the tools are opposite for forward and backward extrusion. With forward extrusion, the contact pressures increase on the extruder plate surface from the axis toward the container surface; on the container surface they increase from the die toward the extruder plate; and on the die surface the increase from the container surface toward its axis (Fig. 7, e). With backward extrusion, the contact pressures on the increase from the container surface toward the surface axis; on the container surface they increase from the extruder plate toward the die; and on the die surface they increase from the working belt toward the container surface.

The maximum pressure values during forward extrusion (765.2 MPa) occur on the extruder plate and container surfaces at the point of their contact. During backward extrusion, these measure 483.3 MPa on the die and container surface at the point of their contact. The forward extrusion maximum design pressure on the die (490.3 MPa) is practically equal to the backward extrusion pressure  $\mu$  (483.3 MPa).

## V. Mean stress in the billet.

The value of the mean stresses and the character of their distribution in the billet being extruded depend on the extrusion technique (Fig.11). During forward extrusion, the value of the mean compressive stresses grows from the axis toward the billet periphery (Fig.11, a) and from the extruder plate toward the die. The maximum compressive stresses in the peripheral area of the billet are 750 MPa. There are tensile

stresses (50 MPa) in the surface layer of the bar as the material exits from the die channel. With backward extrusion and a relative billet length of  $L/D = 1.66$  its stressed state outside the plastic deformation area is heterogeneous: the  $\sigma_m$  value in the area adjacent to the extruder plate is lower (-200 MPa) than at the deformation area inlet (-250 MPa). The maximum compressive stresses occur in the peripheral area of the billet adjacent to the die. The value of the compressive stresses decreases toward the billet. There are tensile stresses (+50 MPa) in the surface layer of the bar at the die exit. These data agrees nicely with the distribution of the contact stresses on the tools (see Fig. 10 and 11). During backward extrusion, the billet field exterior to the plastic deformation area is in a homogeneous stress state, as the billet length reduces (at  $L/D = 1.32$ ).

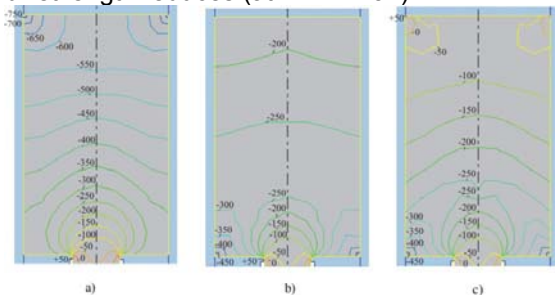


**Figure 11.** Isometric lines of the mean stresses in billets with forward (a), backward (b) and AFF extrusion (c). The butt-end length is 184 mm.

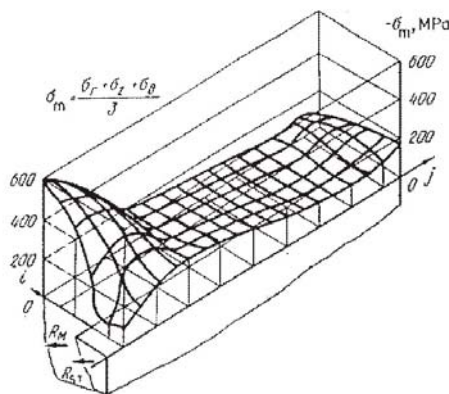


**Figure 12.** Diagram of the mean stresses distribution in backward extrusion. The butt-end length is 184 mm.

During AFF extrusion, the mean stress distribution character in the deformation area is similar to the backward extrusion stress distribution in the initial process step, when active friction forces are still at work. However, the die has a somewhat smaller high-value area and the stresses on the bar surface are equal to zero.

Outside the plastic deformation area, the stresses decrease and in the peripheral billet area they are equal to zero. At this location there is a free billet surface not contacting the container which experiences tensile stresses (+50 MPa). This phenomenon is confirmed both by experimental data and by the fact that after various extrusion stages the extruder plate can be separated from the butt-end virtually without applying any effort. The design character of the  $\sigma_m$  distribution in the billet practically coincides with the results of the studies using the viscoplasticity technique [14] as well (see Fig. 12).

In all extrusion cases the  $\sigma_m$  value in the plastic deformation area decreases toward the die from the maximum value (-350, -250 MPa) to the minimum value (-50 MPa).

The above considerations allow an understanding that the simulation results for the stressed state of a billet reflect the real  $\sigma_m$  distribution in its volume for both AFF and forward/backward extrusion.

## VI. Temperature fields in the billet.

The QForm software makes it possible to obtain the information both on the variation of the temperature field in the billet being extruded, as the process advances and the information on the temperature variations in the individual material points of the billet, which are of interest to the researcher.

Fig. 13 shows the calculated temperature variation in the checkpoints at the die and extruder plate for AFF extrusion at the following conditions: 10 drawing ratio; 380°C billet temperature, 360°C container and extruder plate temperature, 380°C die temperature; 2 mm/s extrusion speed;  $K_V = 1.3$  [15].

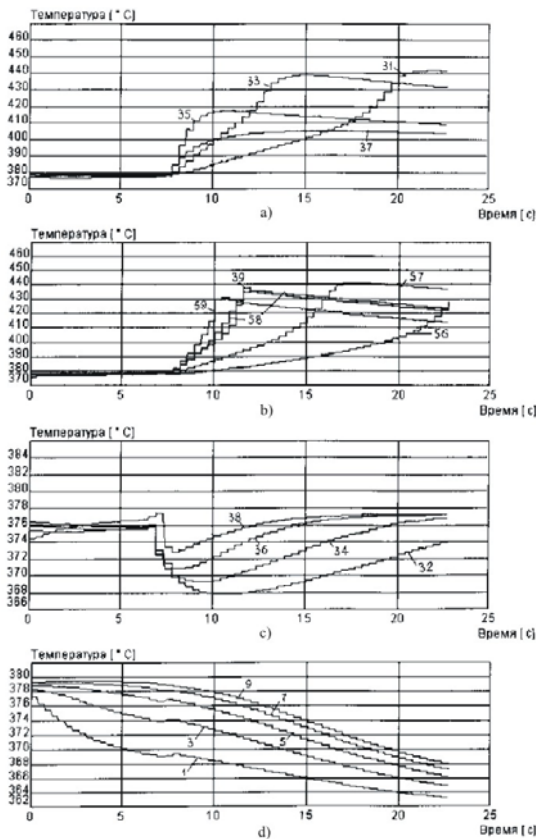


**Figure 13.** Calculated temperature variation in the checkpoints of the billet in the initial AFF extrusion stage [15].

It is evident from Fig. 13 that the temperature increase in the plastic deformation area at the beginning of the process is not uniform being most intensive in the central part of the billet, whereas in the peripheral part it depends on the temperature of the container considerably. The maximum temperatures are observed in the surface layer of the bar exiting the die channel, rather than in the plastic deformation area. The temperature in the remaining volume of the bar is controlled both by the container and extruder plate temperature. If there is a substantial difference in the billet, container and extruder plate temperatures, there is a considerable cooling, even at the beginning of the process, both of the butt portions of the billet at the extruder plate (see Fig. 13) and of the peripheral portion contacting the container. It is evident from Fig. 14 that even at a minor difference in the billet and container temperatures, in the high contact pressure field, the cooling of the billet is more intensive. The shapes of the areas with an elevated temperature of the billet match the shapes and sizes of the plastic deformation area

during forward and backward extrusion (Fig. 19, a, b).

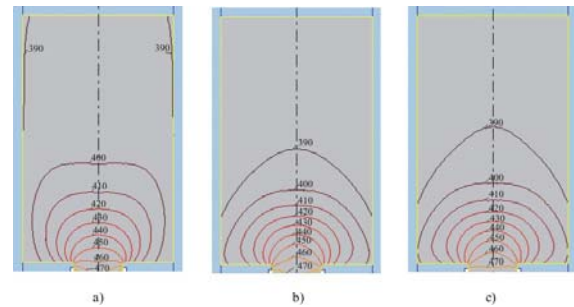


**Figure 14.** Temperature distribution in a billet for forward (a), backward (b) and AFF extrusion under identical temperature and speed conditions (see the simulation conditions) after a 184 mm ram stroke.

## VII. Initial stage AFF extrusion simulation.

These calculations have been made with the aim to verify the possibility of using the QForm software for simulation of various kinematical extrusion conditions. According to the above mentioned recommendations and work results [12, 13, 15], a successful commencement of AFF extrusion for the billets with more than two diameters in length is possible at a certain force pressing out the billet in the container.

Fig. 15 shows the calculation results for two options of the process commencement: when pressing out ram billets in a fixed container using a 5.2 MN force (Fig. 20, a) and a 0.73 MN force (Fig. 15, c).

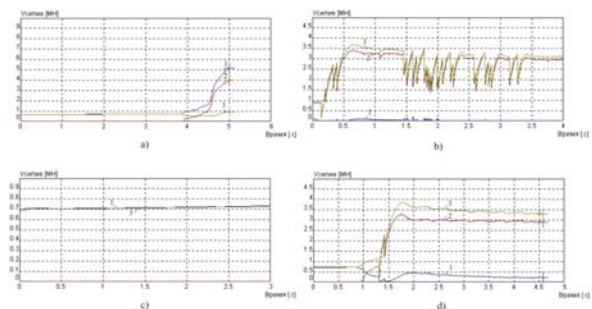


**Figure 15.** Calculated extrusion diagrams (b,d) with pre-determined movement speeds of the ram ( $V_r = 3$  mm/s) and the container ( $V_k = 4.2$  mm/s) for not best suitable (a) and best suitable (c) pressing-out of a billet.

In the former case, by the time the container begins to move (see Fig. 1, c), the billet has been

completely pressed out in the area adjacent to the extruder plate. When the container begins to move, pressing-out of the billet in the area adjacent to the die is completed so the material flow only begins, when it has been pressed out completely, due to the friction forces between the die and the container. This is evidenced by the fact that there is no force at the ram (Fig. 20, b). In these conditions, the onset of the process at the predetermined  $K_V$  factor value is impossible.

In the second case, pressing-out of the billet is complete at the time it touches the container. After the container drive has been switched on, the process begins under the pre-determined kinematical conditions, which is demonstrated by the diagram (Fig. 15, c) typical for AFF extrusion. The AFF extrusion simulation results with the two billet pressing-out options coincide with the results of the experiment [12].

## VIII. Conclusions

1. The QForm software simulates with sufficient accuracy the material flow and force expenditures for the process during extrusion depending on the value and direction of the friction forces between the billet and the container.

2. The calculations results are in agreement with the general provisions about the stressed-and –deformed and thermal state of the billet during forward, backward and active friction force extrusion.

3. The simulation results obtain allow the statement that the QForm finite-element software can be useful to specialists during the process preparation of production and to the research engineers and university students investigating the extrusion process as well.

## IX. References

1. Thomsen E.G., Jang Ch.T., Kobayashi S. Mechanics of plastic deformation in metal processing. New York: Macmillan 1965.

2. Johnson W., Kudo H. The Mechanics of Metal Extrusion. Manchester: Manchester University Press 1962.

3. Flitta I., Sheppard T. On the Mechanics of Friction During the Extrusion Process. 7<sup>th</sup> international aluminum extrusion technology

seminar. Chicago, Illinois, May, 2000, p.p. 197-203.

4. Bandar A.R., Negvesky L., Misiolek W.Z., Kazanowski P. Physical and Numerical Modeling of Billet Upsetting. 7<sup>th</sup> international aluminum extrusion technology seminar. Chicago, Illinois, May, 2000, p.p. 159-166.

5. Thackray R., Dashwood R., McShane H. Simulation of the Effect of Tooling and Billet Condition on Bulk and Surface Metal Flow during Extrusion. 7<sup>th</sup> international aluminum extrusion technology seminar. Chicago, Illinois, May, 2000, p.p. 213-223.

6. Flitta I., Sheppard T. Investigation of friction during the extrusion of Al-alloys using FEM simulation. The 5<sup>th</sup> International Esaform Conference of Material Forming. Krakow, Poland. April 2002. p.p. 435-438.

7. Chumachenko Ye.N., Scherba V.N., Chumachenko S.Ye., Sukhanova A.V. Application of a Material Flow Simulation Computer Model for Extrusion Parameters Design. // Metallurgia, 1998. No. 10, p.p. 31-33.

8. Buntoro I.A., Mueller K.B. Overview of various bending methods directly after extrusion process. The 5<sup>th</sup> International Esaform Conference of Material Forming. Krakow, Poland. April 2002. p.p. 443-446.

9. Koop R., Mueller K., Jao Ch. Visoplastische und numerische Erfassung des Materialflusses beim direkten Strangpressen. Aluminium, 1998. Part I. №1/2, Part II. №4. p.p. 248-255.

10. Biba N.V., Stebunov S.A., Petrov P.A., Perfilov V.I. The development of near net shape forming technology using three-dimensional finite element program QForm 2D/3D. The 5<sup>th</sup> International Esaform Conference of Material Forming. Krakow, Poland. April 2002. p.p. 395-398.

11. Berezhnoy V.L., Scherba V.N., Baturin A.I. Extrusion with Active Friction Force, Metallurgia, Moscow, 1988 (in Russian).

12. Moroz B.S., Mueller K.B., Beresowskij B.N. Simulation of the initial stages of extrusion. Aluminum. 2000 Part I. No. 11, p.p. 898-907; Part II. No. 12, p.p. 1060-1065.



13. Moroz B.S., Berezovsky B.N. Deformation Force Features in the Initial Extrusion Phase.// Kuznechno-shtampovochnoye proizvodstvo [Forging & Forming], 1998. No. 10, p.p. 4-7.

14. Okhrimenko Ya.M., Scherna V.N., Yefremov D.B. Study of the Stressed-and-Deformed State of Metals for Active Friction Extrusion. New Metal Forming Processes. Collected MISiS Works, No. 112. Metallurgia Publishers, Moscow, 1979. P.p. 101-106.

15. Moroz B.S. Development of Scientific Methods for Design of Active Friction Force Aluminum Alloys Extrusion Processes. Doctoral degree thesis (Eng.) – Rostov-on-Don, DSTU, 2000. – 384 pgs.

